Universal two-time correlations, out-of-time-ordered correlators, and Leggett-Garg inequality violation by edge Majorana fermion qubits

F. J. Gómez-Ruiz,[1,2,*] J. J. Mendoza-Arenas,[1] F. J. Rodríguez,[1] C. Tejedor,[3] and L. Quiroga[1]

[1]*Departamento de Física, Universidad de los Andes, A.A. 4976, Bogotá, Colombia*

[2]*Department of Physics, University of Massachusetts, Boston, Massachusetts 02125, USA*

[3]*Departamento de Física Teórica de la Materia Condensada and Condensed Matter Physics Center, Universidad Autónoma de Madrid, 28049 Madrid, Spain*

(Received 2 March 2018; revised manuscript received 23 May 2018; published 20 June 2018)

In the present work we propose that two-time correlations of Majorana edge localized fermions constitute a novel and versatile toolbox for assessing the topological phases of one-dimensional open lattices. Using analytical and numerical calculations in the Kitaev model, we uncover universal relationships between the decay of the short-time correlations and a particular family of out-of-time-ordered correlators, which provide direct experimental alternatives to the quantitative analysis of the system regime, either normal or topological. Furthermore, we show that the saturation of two-time correlations possesses features of an order parameter. Finally, we find that violations of Leggett-Garg inequalities can indicate the topological-normal phase transition by looking at different qubits formed by pairing local and nonlocal edge Majorana fermions.

DOI: 10.1103/PhysRevB.97.235134

I. INTRODUCTION

In the last few years, the development of new quantum devices has fueled the search for novel materials and control mechanisms to engineer unprecedented technologies. Along this path, topological systems have been identified as robust entities with potential applications in quantum computation and information processing due to their unusual braiding properties [1–3]. Candidates for topological qubits include chains of magnetic atoms on top of a superconducting surface [4], hybrid systems between s-wave superconductors and topological insulators [5], p-wave superconductors [6], fractional quantum Hall systems [7], and one-dimensional (1D) semiconductor-superconductor heterostructure-based quantum wires [8–10]. Notably, the latter have aroused great interest given their high experimental accessibility and controllability [11]. In addition, edge-localized Majorana zero modes, expected to be robust against dephasing and dissipation [12–15], have been predicted to exist in these systems. The search for new topological configurations allowing for Majorana zero modes has also been extended to Josephson-junction-based nanostructures [16–20]. Concurrent with the chase for novel materials is the search for experimentally accessible properties to identify their truly nonclassical features, such as topological quantum phases. A large number of protocols have been proposed to this end, and a particularly important subset corresponds to those based on spatial nonlocal correlations as embodied in Bell inequalities [13,21,22]. More recently, there has been a surge of theoretical and experimental interest in using temporal correlations instead for similar purposes since in some scenarios nonlocal measurements are quite challenging. Thus, local measurements such as two-time correlations (TTCs) can be used to gain further access to the underlying physics [23,24].

Here we consider an extension of that interest to assess the interplay between time correlations and nonlocal quantum objects in Majorana fermion chains by focusing mainly on the Kitaev chain [25]. In particular we address the open question of detecting true quantum temporal correlations in a topological quantum phase. Correlations for two types of objects will be explored: (i) local Dirac fermions formed by pairing two Majorana fermions on the same edge site and (ii) nonlocal Dirac fermions coming from the pairing of Majorana fermions located at the two opposed edge sites of the chain. In this way we will address the pivotal role that TTCs play in detecting large memory effects of local and nonlocal Majorana edge qubits.

Specifically, we will show how the longtime limit of several boundary TTCs possesses features of an order parameter, providing information on the quantum phase transitions of the Majorana fermion system. Moreover, for the purposes of the present work, TTCs can be used to assess the quantumness of a system in a form similar to how spatial correlations identify quantum behavior through Bell inequalities. Namely, combinations of TTCs allow for testing Leggett-Garg inequalities (LGIs) [26–28]. These inequalities are satisfied in macroscopic classical systems, characterized by macrorealism (a system's property is well defined at every time regardless of whether it is observed) and noninvasive measurability (a system is unaffected by measurements). Their violation indicates the existence of macroscopic quantum coherence.

Not only has there been an intense search for experimental schemes in which LGI violations can be observed [29–36], but several applications for them have also been proposed, including identification of order-disorder quantum phase transitions in many-body systems [37] and characterization of quantum transport [38]. Indeed, it is also interesting to extend the range

*fj.gomez34@uniandes.edu.co

of LGI violation features as a detection tool for topological phase transitions. Along this line, our results provide a first step for understanding the link between correlations in space and time domains in a concrete topological condensed-matter setup. Moreover, we stress that all of our results remain valid for an edge spin in the transverse field Ising open chain by applying a Jordan-Wigner transformation to the open Kitaev chain model.

This paper is organized as follows. Section II gives a brief review of specific Majorana fermion chains (in the language of the 1D Kitaev model), their exact diagonalization, and theoretical aspects of Majorana qubit two-time correlations. In Sec. III numerical results of Majorana-qubit-TTC behavior for short-, intermediate-, and long-time regimes are discussed. In Sec. IV a brief recap of LGI is given, with a focus on the intermediate-time regime. Both analytical and numerical results are provided and contrasted whenever possible. Section V is devoted to possible experimental implementations where TTC and LGI behaviors of Majorana-based qubits could be tested. Finally, in Sec. VI we present a summary of this work.

II. THEORETICAL FRAMEWORK

A. Majorana fermion chain

We focus on a concrete realization of a Majorana fermion chain in terms of the Kitaev model [25]. It is described by the Hamiltonian

$$\hat{H} = -\frac{\mu}{2}\sum_{j=1}^{N}(2\hat{n}_j - 1) - \omega\sum_{j=1}^{N-1}(\hat{c}_j^\dagger\hat{c}_{j+1} + \hat{c}_{j+1}^\dagger\hat{c}_j) + \Delta\sum_{j=1}^{N-1}(\hat{c}_j\hat{c}_{j+1} + \hat{c}_{j+1}^\dagger\hat{c}_j^\dagger), \tag{1}$$

representing a system of noninteracting spinless fermions on an open-end chain of N sites labeled by $j = 1,\ldots,N$. The single-site fermion occupation operator is denoted by $\hat{n}_j = \hat{c}_j^\dagger\hat{c}_j$; the chemical potential is μ, taken to be uniform along the chain; ω is the hopping amplitude between nearest-neighbor sites [we assume $\omega \geqslant 0$ without loss of generality because the case with $\omega \leqslant 0$ can be obtained by a unitary transformation: $\hat{c}_j \to -i(-1)^j\hat{c}_j$]; and Δ is the p-wave paring gap, which is assumed to be real, with $\Delta \geqslant 0$ (the case $\Delta \leqslant 0$ can be obtained by the transformation $\hat{c}_j \to i\,\hat{c}_j$ for all j). This model captures the physics of a 1D topological superconductor with a phase transition between topological and nontopological (trivial) phases at $\mu = 2\Delta$ for $\Delta = \omega$. Notice that for this symmetric hopping-pairing Kitaev Hamiltonian, i.e., $\omega = \Delta$, a Jordan-Wigner transformation leads directly to the transverse field Ising model [39]. Thus, from now on we will refer to the Majorana fermion chain as either the Kitaev chain or the transverse field Ising model.

Let us introduce Majorana operators $\hat{\gamma}_j$ to express the real-space spinless fermion annihilation and creation operators as

$$\hat{c}_j = \tfrac{1}{2}(\hat{\gamma}_{2j-1} + i\hat{\gamma}_{2j}), \quad \hat{c}_j^\dagger = \tfrac{1}{2}(\hat{\gamma}_{2j-1} - i\hat{\gamma}_{2j}). \tag{2}$$

These are Hermitian operators ($\hat{\gamma}_j = \hat{\gamma}_j^\dagger$), satisfy the property $(\hat{\gamma}_j)^2 = (\hat{\gamma}_i^\dagger)^2 = 1$, and obey the modified anticommutation relations $\{\hat{\gamma}_i,\hat{\gamma}_j\} = 2\delta_{i,j}$, with $i,j = 1,\ldots,2N$. From the definition of Majorana operators (2) it is evident that for each spinless fermion on site j, two Majorana fermions are assigned to that site, denoted by $\hat{\gamma}_{2j-1}$ and $\hat{\gamma}_{2j}$. They allow the Kitaev Hamiltonian in Eq. (1) to be written in the equivalent form:

$$\hat{H} = -i\frac{\mu}{2}\sum_{j=1}^{N}\hat{\gamma}_{2j-1}\hat{\gamma}_{2j} + \frac{i}{2}\sum_{j=1}^{N-1}[(\omega+\Delta)\,\hat{\gamma}_{2j}\hat{\gamma}_{2j+1} - (\omega-\Delta)\,\hat{\gamma}_{2j-1}\hat{\gamma}_{2j+2}]. \tag{3}$$

In order to put the Majorana fermion Hamiltonian in Eq. (1) [or, equivalently, in Eq. (3)] in diagonal form, a standard Bogoliubov transformation (see the Supplemental Material (SM) [40]) is performed:

$$\begin{aligned}\hat{c}_j^\dagger &= \sum_{k=1}^{N}(u_{2k,j}\hat{d}_k + v_{2k,j}\hat{d}_k^\dagger),\\ \hat{c}_j &= \sum_{k=1}^{N}(u_{2k,j}\hat{d}_k^\dagger + v_{2k,j}\hat{d}_k),\end{aligned} \tag{4}$$

where k denotes a single-fermion mode, $u_{2k,j}$ and $v_{2k,j}$ are real numbers, and the canonical fermion anticommutation relations for the new operators $\hat{d}_k$ and $\hat{d}_k^\dagger$ remain true, that is, $\{\hat{d}_k,\hat{d}_{k'}^\dagger\} = \delta_{k,k'}$, $\{\hat{d}_k^\dagger,\hat{d}_{k'}^\dagger\} = \{\hat{d}_k,\hat{d}_{k'}\} = 0$. Thus, the exact diagonalization of the Kitaev Hamiltonian in Eq. (1), in terms of the new independent fermion mode operators $\hat{d}(\hat{d}^\dagger)$, leads to

$$\hat{H} = \sum_{k=1}^{N}\epsilon_k\left[\hat{d}_k^\dagger\hat{d}_k - \frac{1}{2}\right], \tag{5}$$

where the new fermion mode energies $\epsilon_k \geqslant 0$ are to be numerically calculated for a Kitaev chain with open ends (although analytical exact results may be found in some cases; see [41]). The matrix representation of Eq. (5) is explicitly written in the SM [40].

B. Two-time correlations

The key quantity of interest in the present work is the symmetrized TTC $\mathcal{C}(t_1,t_2)$, as given by the expression [37]

$$\mathcal{C}(t_1,t_2) = \tfrac{1}{2}\langle\{\hat{Q}(t_2),\hat{Q}(t_1)\}\rangle, \tag{6}$$

where $\hat{Q}$ denotes a single-qubit operator (a dichotomic observable, i.e., with eigenvalues $q = \pm 1$) to be specified later, $\{\hat{Q},\hat{Q}'\}$ is an anticommutator, and $\hat{Q}(t_n)$ is the qubit operator at time t_n. Since the TTC is to be evaluated for stationary states, it does not depend on the individual times t_1 and t_2, only on their difference $t = t_2 - t_1$, leading simply to $\mathcal{C}(t_1,t_2) = \mathcal{C}(t,0) = \mathcal{C}(t)$.

In the following sections, we present an analytical approach for the evaluation of TTCs for single- and double-Majorana qubits, together with extensive supporting numerical data. In particular in Sec. II C we obtain the early-time TTC behavior for different local and nonlocal qubits, demonstrating that for the local single- and double-Majorana-qubit cases universal features (independent of the chain quantum state itself, as

well as chain size) can be identified, providing local information about the global-system many-body quantum phase. We also link the TTCs short-time evolution to a special kind of recently established many-time correlator, the so-called out-of-time-ordered correlators, which are gaining growing interest. Moreover, in Sec. II D we provide analytical results for single- and double-Majorana TTCs for arbitrary times, showing how the former serves as a test of topological criticality by directly indicating the existence of edge-localized zero-energy modes. These results are then fully evaluated numerically in Sec. III.

C. TTC short-time behavior and out-of-time-ordered correlation function

In order to assess the sensitivity of TTCs for detecting quantum phase transitions by looking at a single local site, we connect the short-time TTC behavior to a second-order expansion with the out-of-time-ordered correlation function $\mathcal{T}(t) = \langle \hat{O}_1^\dagger(t)\hat{O}_2^\dagger(0)\hat{O}_1(t)\hat{O}_2(0)\rangle$ [42–45]. Let us expand up to second order in time the TTC as given by Eq. (6), yielding

$$\begin{aligned}\mathcal{C}(t) &= \frac{1}{2}\langle\{e^{i\hat{H}t}\hat{Q}e^{-i\hat{H}t},\hat{Q}\}\rangle \\ &\simeq 1 - \frac{t^2}{2}\langle -[\hat{H},\hat{Q}]^2\rangle + O(t^4). \end{aligned} \tag{7}$$

Note that the second line in the above equation holds for any single-site qubit observable $\hat{Q}$ such that $\hat{Q}^2 = \hat{1}$, evolving under the action of an arbitrary (local or global) Hamiltonian $\hat{H}$. Moreover, and most interestingly, the first line in Eq. (7) is nothing but the real part of the $\mathcal{T}(t)$ corresponding to a Hermitian single-qubit operator $\hat{O}_2 = \hat{Q}$ and the unitary operator $\hat{O}_1(t) = e^{-i\hat{H}t}$.

First, let us consider the TTC for a single-edge Majorana fermion $j = 1$, i.e., $\hat{Q} = \hat{\gamma}_1$. By resorting to Eq. (3) it is easy to check that $[\hat{H},\hat{\gamma}_1]^2 = -\mu^2$, a scalar quantity, thus producing for the real part of the corresponding $\mathcal{T}(t)$ the simple and universal result $\langle -[\hat{H},\hat{\gamma}_1]^2\rangle = \mu^2$, valid for any Majorana fermion chain pure state $|\psi_K\rangle$ or mixed state $\hat{\rho}_K$. Note that via the Jordan-Wigner transformation, this qubit operator corresponds to $\hat{\sigma}_1^x$ for the transverse field Ising model, i.e., $\hat{\gamma}_1 = \hat{\sigma}_1^x$, the x-spin operator of an edge chain site. Consequently, we rewrite the TTC in Eq. (7) as $\mathcal{C}_1^{(x)}(t)$,

$$\mathcal{C}_1^{(x)}(t) = \frac{1}{2}\langle\{\hat{\gamma}_1(t),\hat{\gamma}_1\}\rangle \simeq 1 - \frac{\mu^2}{2}t^2 + O(t^4). \tag{8}$$

As a second case, we consider a two-Majorana edge qubit such as $\hat{Q} = 2\hat{n}_1 - \hat{1} = -i\,\hat{\gamma}_1\hat{\gamma}_2$. This qubit corresponds, via the Jordan-Wigner transformation, to the $\hat{\sigma}_1^z$ edge spin operator for the transverse field Ising model, i.e., $-i\,\hat{\gamma}_1\hat{\gamma}_2 = \hat{\sigma}_1^z$. Now it is straightforward to show that $[\hat{H},-i\,\hat{\gamma}_1\hat{\gamma}_2]^2 = -4\Delta^2$, again a scalar quantity, hence producing a result valid for any Majorana fermion chain pure state $|\psi_K\rangle$ or mixed state $\hat{\rho}_K$. Thus, the second derivative of the real part of $\mathcal{T}(t)$ reduces to the universal value $\langle -[\hat{H},-i\,\hat{\gamma}_1\hat{\gamma}_2]^2\rangle = 4\Delta^2$, and consequently, the short-time expression for $\mathcal{C}_1^{(z)}(t)$ becomes

$$\begin{aligned}\mathcal{C}_1^{(z)}(t) &= -\tfrac{1}{2}\langle\{\hat{\gamma}_1(t)\hat{\gamma}_2(t),\hat{\gamma}_1\hat{\gamma}_2\}\rangle \\ &\simeq 1 - 2\Delta^2 t^2 + O(t^4). \end{aligned} \tag{9}$$

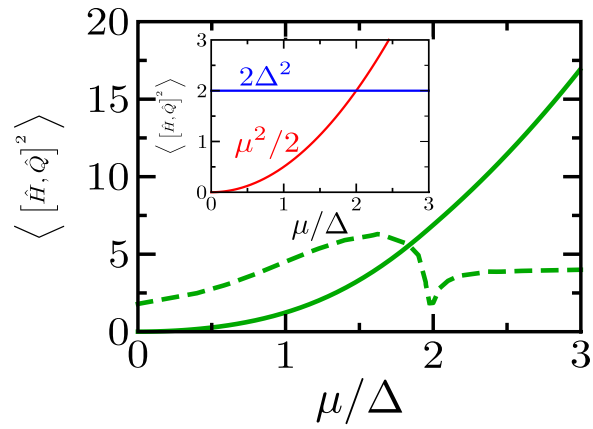

FIG. 1. Short-time curvature for the nonlocal two-Majorana qubit $\mathcal{C}_{1,N}(t)$ (green solid line) and its second derivative with respect to μ (green dashed line), as a function of μ/Δ. The latter presents a clear dip at the topological quantum critical point. Inset: TTC initial curvature for local Majorana qubits, $\mathcal{C}_1^x(t)$ (red line) and $\mathcal{C}_1^z(t)$ (blue line), showing a crossing just at the critical point.

As a third case, we analyze the short-time behavior of the nonlocal Dirac fermion formed by coupling two Majorana operators located at the two edges of the chain, $\hat{Q}_{1,N} = i\,\hat{\gamma}_1\hat{\gamma}_{2N}$. The expansion of the corresponding TTC leads to

$$\begin{aligned}\mathcal{C}_{1,N}(t) &= -\tfrac{1}{2}\langle\{\hat{\gamma}_1(t)\hat{\gamma}_{2N}(t),\hat{\gamma}_1\hat{\gamma}_{2N}\}\rangle \\ &\simeq 1 - \mu^2(1 - \langle\hat{\gamma}_1\hat{\gamma}_2\hat{\gamma}_{2N-1}\hat{\gamma}_{2N}\rangle)\,t^2 + O(t^4). \end{aligned} \tag{10}$$

It is evident that this TTC features a nonuniversal short-time evolution, given that it depends on the specific quantum state of the Majorana fermion chain. This is indicated by the expected value of the four-Majorana-operator term $\langle\hat{\gamma}_1\hat{\gamma}_2\hat{\gamma}_{2N-1}\hat{\gamma}_{2N}\rangle = \langle\hat{\gamma}_1\hat{\gamma}_2\rangle\langle\hat{\gamma}_{2N-1}\hat{\gamma}_{2N}\rangle + \langle\hat{\gamma}_1\hat{\gamma}_{2N}\rangle\langle\hat{\gamma}_2\hat{\gamma}_{2N-1}\rangle$, which for a sufficiently long chain can be approximated to $\langle\hat{\gamma}_1\hat{\gamma}_2\hat{\gamma}_{2N-1}\hat{\gamma}_{2N}\rangle \simeq \langle\hat{\gamma}_1\hat{\gamma}_2\rangle^2$ in the ground state.

In Fig. 1 the short-time curvature (second time derivative) of the edge TTCs corresponding to single- and double-Majorana fermions is depicted as a function of μ/Δ. In the main panel the nonlocal case of $\mathcal{C}_{1,N}(t)$ is plotted (solid line), while in the inset those of $\mathcal{C}_1^{(x)}(t)$ and $\mathcal{C}_1^{(z)}(t)$ are depicted. Clearly, by comparing Eqs. (8) and (9), a universal crossing of initial TTC curvatures occurs for $\mu = 2\Delta$, which signals the critical point for the topological-trivial phase transition in the Kitaev model, or, equivalently, for the ferromagnetic-paramagnetic transition in the transverse field Ising model. This remarkable universal behavior, i.e., the independence from the Majorana fermion chain quantum state, holds true only for the edge sites of both these models as realized by the Kitaev chain and transverse field Ising systems. By contrast, the nonlocal $\mathcal{C}_{1,N}(t)$ shows a nonuniversal behavior depending on the specific quantum state of the Majorana fermion chain. The results plotted in the main panel of Fig. 1 have been obtained numerically, as explained below, for a Kitaev chain in the ground state. In the same panel the second derivative of the curvature with respect to μ is also plotted (dashed line), which clearly presents a dip at the critical point $\mu/\Delta = 2$. Thus, we observe that the

early-time correlators, with both universal and nonuniversal behavior, are sensitive to the topological phase transition.

D. General two-time correlation behavior of Majorana qubits

Having established the relevance of TTCs and a related family of out-of-time-ordered correlations for edge sites in the Majorana fermion chain, we proceed to explore the TTC behavior for qubits formed by any combination of edge and/or bulk sites for arbitrary times. By developing the Majorana qubits in terms of Bogoliubov operators (see SM [40]) we proceed to express both the single- and double-Majorana TTCs in convenient forms for numerical analysis. We follow the same notation for Bogoliubov coefficients used in Ref. [46]. As we discuss below, this numerical procedure is essential to further progress, except in special cases for $\mathcal{C}_1^{(x)}(t)$ where an exact closed form has been obtained.

1. Single-Majorana edge two-time correlations

First, we note that the $\mathcal{C}_1^{(x)}(t)$ TTC admits a universal exact closed expression for arbitrary pure or mixed quantum states of the Majorana fermion chain (see SM [40]). We found that

$$\mathcal{C}_1^{(x)}(t) = \sum_{m=0}^{\infty} \frac{(-1)^m}{(2m)!}(2\Delta t)^{2m}\mathcal{N}_m(u^2), \tag{11}$$

where $u = \frac{\mu}{2\Delta}$ and $\mathcal{N}_m(x) = \sum_{n=1}^{m} N_{m,n}x^n$ are the well-known Narayana polynomials, which involve the Narayana numbers $N_{m,n} = \frac{1}{m}\binom{m}{n-1}\binom{m}{n}$ [47,48]. Note that the critical point corresponds to $u = 1$, for which $\mathcal{N}_m(1) = C_m = \frac{1}{m+1}\binom{2m}{m}$, the most famous Catalan numbers. Importantly, Eq. (11) can be calculated in a closed form at the critical point $u = 1$, yielding the simple expression

$$\mathcal{C}_1^{(x)}(t) = \frac{\mathcal{J}_1(4\Delta t)}{2\Delta t} \tag{12}$$

in terms of the Bessel function of the first kind $\mathcal{J}_1(z)$. To the best of our knowledge this compact result has not been discussed neither in the literature on the Ising nor in that of the Kitaev model. We emphasize that the expressions given by Eqs. (11) and (12) are always valid, and thus, they are of universal reach, independent of the pure or mixed state of the Majorana fermion chain. Consequently, they hold true even at infinite temperature.

For other values of u such a simple form has yet to be found. However, the analytics can be developed further, leading to deeper insights on the general behavior of the TTCs. First, Eq. (11) allows for establishing a link of $\mathcal{C}_1^{(x)}(t)$ TTC on both phases around the critical point $u = 1$, which will come in handy afterwards. Since the Narayana polynomials are symmetric, the property $\mathcal{N}_m(\frac{1}{x}) = \frac{1}{x^{m+1}}\mathcal{N}_m(x)$ holds. Consequently,

$$\mathcal{C}_1^{(x)}\left(t, \frac{1}{u}\right) = 1 - \frac{1}{u^2} + \frac{1}{u^2}\,\mathcal{C}_1^{(x)}\left(\frac{t}{u}, u\right), \tag{13}$$

indicating that the x TTC behaves in one phase (reduced chemical potential $\frac{1}{u}$) as it would in the complementary phase (reduced chemical potential u) but with a scaled time $\frac{t}{u}$.

Furthermore, for numerical calculations the time evolution of a single-Majorana-edge-fermion operator, $\hat{\gamma}_i(t) = e^{i\hat{H}t}\hat{\gamma}_i(0)e^{-i\hat{H}t}$, is found to be

$$\begin{aligned}\hat{\gamma}_{2j-1}(t) &= \sum_{m=1}^{N}\{\hat{\gamma}_{2m-1}\, g_{m,j}^{(+,+)}(t) + \hat{\gamma}_{2m}\, h_{m,j}^{(-,+)}(t)\},\\ \hat{\gamma}_{2j}(t) &= \sum_{m=1}^{N}\{\hat{\gamma}_{2m}\, g_{m,j}^{(-,-)}(t) - \hat{\gamma}_{2m-1}\, h_{m,j}^{(+,-)}(t)\},\end{aligned} \tag{14}$$

where

$$\begin{aligned} g_{m,j}^{(\nu,\nu)}(t) &= \sum_k \cos(\epsilon_k\, t)\,(u_{2k,m} + \nu v_{2k,m})\,(u_{2k,j} + \nu v_{2k,j}),\\ h_{m,j}^{(\nu,-\nu)}(t) &= \sum_k \sin(\epsilon_k\, t)\,(u_{2k,m} - \nu v_{2k,m})\,(u_{2k,j} + \nu v_{2k,j}),\end{aligned} \tag{15}$$

with $\nu = +,-$. A direct application of these relations allows us to obtain an analytical expression for the full time evolution of $\mathcal{C}_1^{(x)}(t)$ as

$$\mathcal{C}_1^{(x)}(t) = \sum_k \cos(\epsilon_k\, t)(u_{2k,1} + v_{2k,1})^2, \tag{16}$$

where $\langle\gamma_{2i}\gamma_{2j-1}\rangle = -i\sum_k (u_{2k,i} - v_{2k,i})(u_{2k,j} + v_{2k,j})$ and $\langle\gamma_{2i}\gamma_{2j}\rangle = \langle\gamma_{2i-1}\gamma_{2j-1}\rangle = \delta_{i,j}$ have been used. By expanding Eq. (16) up to second order in time and comparing it with the universal result quoted in Eq. (8), the following identity holds true:

$$\sum_k \epsilon_k^2\,(u_{2k,1} + v_{2k,1})^2 = \mu^2, \tag{17}$$

which is valid for open Kitaev and transverse field Ising models (with μ replaced by the transverse magnetic field) of arbitrary chain length. The identity given by Eq. (17) provides by itself a consistency check of numerical calculations.

Now let us look at the long-time limit of $\mathcal{C}_1^{(x)}(t)$ by averaging Eq. (16) over a long time period. As the time average of $\cos(\epsilon_k\, t)$ vanishes unless some fermion mode has energy $\epsilon_M = 0$, i.e., a zero-energy Majorana mode exists (for which the average is 1), we can readily ensure that for the topological regime

$$\lim_{t\to\infty} \mathcal{C}_1^{(x)}(t) \simeq (u_{M,1} + v_{M,1})^2 = 4u_{M,1}^2 \tag{18}$$

since $u_{M,1} = v_{M,1}$, i.e., the electron and hole contributions for the zero-energy Majorana mode $k = M$ at site $j = 1$ are the same. Consequently, we propose that a measurement of the long-time saturation value of the edge $\mathcal{C}_1^{(x)}$ TTC provides a witness of the topological ($\neq 0$) and nontopological ($= 0$) phase transition of the Majorana fermion chain systems, as it probes directly the existence of zero-energy modes. Additionally, it gives direct access to the electron-hole weight of such modes.

2. Two-time correlations of double-Majorana qubits

We focus now on qubits formed by any pair of Majorana fermions such as $\hat{\gamma}_{2i-1}$ and $\hat{\gamma}_{2j}$; details of the calculations are given in the SM [40]. We define

$$\hat{\theta}_{i,j} = \tfrac{1}{2}(\hat{\gamma}_{2i-1} + i\,\hat{\gamma}_{2j}), \quad \hat{\theta}_{i,j}^{\dagger} = \tfrac{1}{2}(\hat{\gamma}_{2i-1} - i\,\hat{\gamma}_{2j}). \tag{19}$$

Notice that $i = j$ implies that the forming Majorana modes are located on the same physical site, and the Kitaev operators in

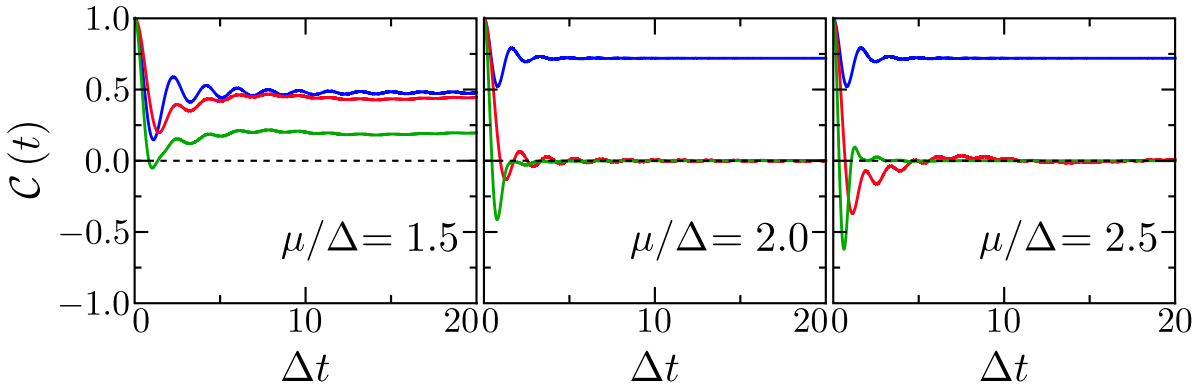

FIG. 2. Edge single- and double-Majorana-qubit TTC in the topological phase ($\mu/\Delta = 1.5$, left panel), at the transition point ($\mu/\Delta = 2$, middle panel), and in the nontopological phase ($\mu/\Delta = 2.5$, right panel). In all panels the red line depicts the $\mathcal{C}_1^{(x)}(t)$ TTC, the blue line represents the $\mathcal{C}_1^{(z)}(t)$ TTC, and the green line corresponds to $\mathcal{C}_{1,N}(t)$.

Eq. (1) are recovered, i.e., $\hat{\theta}_{j,j} = \hat{c}_j$. On the other hand, for $i \neq j$ the Majorana fermions are located on different physical sites. It is easy to check that the usual Dirac fermion relations hold true for operators $\hat{\theta}_{i,j}$ and $\hat{\theta}_{i,j}^\dagger$ as $\{\hat{\theta}_{i,j}, \hat{\theta}_{i,j}^\dagger\} = 1$, $\{\hat{\theta}_{i,j}^\dagger, \hat{\theta}_{i,j}^\dagger\} = \{\hat{\theta}_{i,j}, \hat{\theta}_{i,j}\} = 0$. Thus, we can define nonlocal Majorana qubits as $\hat{Q}_{i,j} = 2\hat{\theta}_{i,j}^\dagger \hat{\theta}_{i,j} - 1$, which have eigenvalues ± 1. Expressing $\hat{Q}_{i,j}(t) = \frac{1}{2}[\hat{\gamma}_{2i-1}(t) - i\,\hat{\gamma}_{2j}(t)][\hat{\gamma}_{2i-1}(t) + i\,\hat{\gamma}_{2j}(t)] - 1 = \frac{1}{2}[\hat{c}_i(t) + \hat{c}_i^\dagger(t), \hat{c}_j(t) - \hat{c}_j^\dagger(t)]$ in terms of commutators of diagonal fermionic mode operators, it becomes possible to evaluate the corresponding TTC not only for the ground state but for any excited eigenstate $|\psi_K\rangle$ of the Kitaev chain. The TTC for general Majorana qubits turns out to be

$$\begin{aligned}\mathcal{C}_{i,j}(t) = 1 - \sum_{k=1}^{N}\sum_{q=1}^{N}\Bigg\{ &\sin^2\left(\frac{\epsilon_k + \epsilon_q}{2}t\right)[(u_{2k,i} + v_{2k,i}) \\ &\times (u_{2q,j} - v_{2q,j}) - (u_{2q,i} + v_{2q,i})(u_{2k,j} - v_{2k,j})]^2 \\ &\times [1 - (n_q - n_k)^2] + \sin^2\left(\frac{\epsilon_k - \epsilon_q}{2}t\right)[(u_{2k,i} + v_{2k,i}) \\ &\times (u_{2q,j} - v_{2q,j}) + (u_{2q,i} + v_{2q,i})(u_{2k,j} - v_{2k,j})]^2 \\ &\times (n_q - n_k)^2\Bigg\}, \end{aligned} \tag{20}$$

where $n_k = 0$ denotes the kth fermion mode is empty, while $n_k = 1$ means it is occupied. By focusing on the edge TTC, i.e., $i = j = 1$ and $\mathcal{C}_{1,1}(t) = \mathcal{C}_1^{(z)}(t)$, expanding the right-hand side of Eq. (20) up to second order in time, and comparing it to the universal result quoted in Eq. (9), a new identity results:

$$\sum_{k=1}^{N}\sum_{q=1}^{N}(\epsilon_k + \epsilon_q)^2(u_{2k,1}v_{2q,1} - u_{2q,1}v_{2k,1})^2 = 2\Delta^2, \tag{21}$$

which is valid for both open-boundary Kitaev and transverse field Ising models (with Δ replaced by the spin-exchange interaction) for arbitrary chain lengths. Like before, the identity given by Eq. (21) turns out to be another important consistency check for numerical calculations.

III. RESULTS AND DISCUSSION

Now we evaluate numerically the different time correlations discussed in Sec. II D. All the results we describe below correspond to an open-ended Majorana fermion chain with $N = 101$ sites in the many-body ground state, $|\psi_K\rangle = \bigotimes_{k=1}^{N}|0\rangle$, with symmetric hopping-pairing energies, i.e., $\omega = \Delta = 1$, which also fixes the energy scale. Their inverse fixes the timescale through the dimensionless variable Δt. In Fig. 2 the time evolution of both single-Majorana edge qubits $\mathcal{C}_1^{(x)}(t)$ and two-Majorana edge qubits $\mathcal{C}_1^{(z)}(t)$ and $\mathcal{C}_{1,N}(t)$ is displayed for three specific values of the chemical potential, namely, $\mu/\Delta = 1.5$ (left panel), $\mu/\Delta = 2.0$ (middle panel), and $\mu/\Delta = 2.5$ (right panel). Oscillatory features are dominant for both short- and intermediate-time regimes $\Delta t < 10$, which subsequently are attenuated until the TTCs reach stationary or asymptotical values for $\Delta t > 10$. We first discuss this long-time regime.

It can be seen that the asymptotic behaviors of $\mathcal{C}_1^{(x)}(t)$ and $\mathcal{C}_{1,N}(t)$ TTCs are very different from that of $\mathcal{C}_1^{(z)}(t)$ TTC crossing the critical point to the trivial phase. We found that these three TTCs remain finite in the topological phase even at infinite time, which agrees with the numerically based observation in Ref. [49] that long coherence times for edge sites in open-boundary Majorana fermion chains are possible. However, the long-time limits of $\mathcal{C}_1^{(x)}(t)$ and $\mathcal{C}_{1,N}(t)$ vanish when the system enters the nontopological or trivial phase [$\mathcal{C}_1^{(z)}(t)$ saturates to finite values at both phases]. This order-parameter-like behavior of the TTC long-time limit is displayed in Fig. 3. Furthermore, by both numerical fitting and the exact general duality property expressed in Eq. (13), we establish that the long-time limit of the single-Majorana edge $\mathcal{C}_1^{(x)}(t)$ TTC has a simple specific functional behavior given by

$$\lim_{t\to\infty}\mathcal{C}_1^{(x)}(t) = \begin{cases} 1 - \left(\frac{\mu}{2\Delta}\right)^2 & \text{for } \mu < 2\Delta, \\ 0 & \text{for } \mu > 2\Delta. \end{cases} \tag{22}$$

On the other hand, the decay of the limit value of the nonlocal $\mathcal{C}_{1,N}(t)$ TTC as a function of μ/Δ has been evaluated numerically, showing a gradual transition, instead of an abrupt one, from one phase to the other. Note that these results are strictly valid for an infinitely long chain or for times below

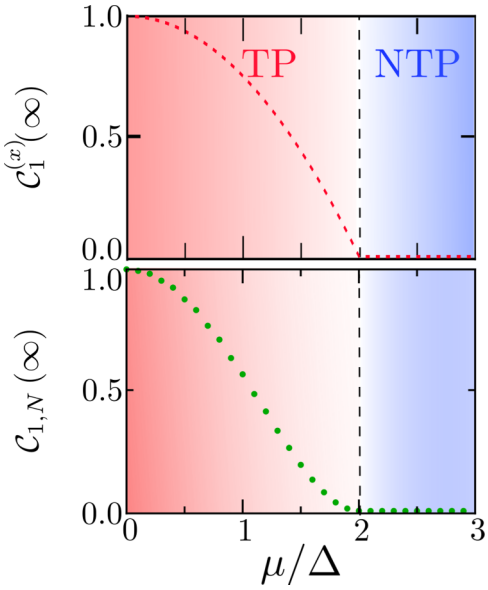

FIG. 3. Long-time limits of edge TTCs as a function of μ/Δ: single-Majorana edge $\mathcal{C}_1^{(x)}(t)$ TTC (top) and nonlocal double-Majorana edge $\mathcal{C}_{1,N}(t)$ TTC (bottom). The order-parameter-like behavior exhibited by the long-time limits is evident. TP: topological phase, NTP: nontopological phase.

a certain limit where finite-size effects could emerge, such as possible interference or revivals coming from the reflected influence of the other edge (not shown here). In addition, the quantum behavior of single-site TTCs for the edge single- and double-Majorana qubits is similar to the x and z spin correlations of the transverse Ising model, and consequently, its quantum critical point could also be detected by TTC measurements [37].

Finally, we end this section with a comparison between edge and bulk TTCs. In Fig. 4 the short- and intermediate-time behaviors of the $\mathcal{C}_{i,j}(t)$ TTC are illustrated for edge Majorana qubits, namely, the local case $i,j=1$ and the nonlocal case $i,j=1,N$, and a bulk two-Majorana qubit $i,j=\frac{N+1}{2},\frac{N+1}{2}$. We conclude that apart from a different oscillation amplitude, the local two-Majorana TTCs, located either at the edge or at a bulk site, are very similar in going to a finite long-time limit in any phase; thus we are not able to detect such a phase transition by looking at that specific feature. This behavior contrasts with that of the two-Majorana nonlocal edge TTC and even, as discussed above, with that shown by the single-Majorana edge TTC. Next, we focus on the consequences of these TTC features when assessing macroscopic quantum coherence through the Leggett-Garg inequality violations by both local- and nonlocal TTCs.

IV. LEGGETT-GARG INEQUALITY

Leggett and Garg [26,27] showed that temporal correlations obey inequalities similar to those of spatial nonlocal measurements such as those performed in a Bell inequality test setup. They approached this by first codifying our intuition about the macroscopic world into three principles:

(i) *Macroscopic realism.* A system's property is well defined at every time regardless of whether or not it is observed.

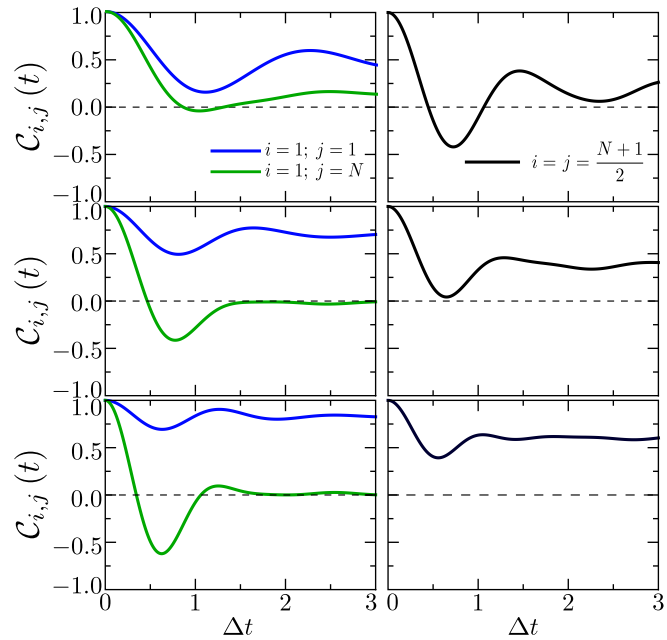

FIG. 4. $\mathcal{C}_{i,j}(t)$ TTC as a function of the dimensionless time Δt in the short- and intermediate-time regimes. Left panels display the TTCs for *two-Majorana qubits*; the blue (green) line shows the $\mathcal{C}_{1,1}(t)=\mathcal{C}_1^{(z)}(t)$ local TTC [$\mathcal{C}_{1,N}(t)$ nonlocal TTC]. Right panels illustrate the time evolution behavior of TTCs for a local *bulk* two-Majorana qubit [middle site of the Majorana fermion chain $\mathcal{C}_{\frac{N+1}{2},\frac{N+1}{2}}(t)$]. The chemical potentials are $\mu/\Delta=1.5$ (top), $\mu/\Delta=2.0$ (middle), and $\mu/\Delta=2.5$ (bottom).

(ii) *Noninvasive measurability.* The system's evolution is unaffected by measurements taken on it.

(iii) *Arrow of time.* The outcome of a measurement cannot be affected by a subsequent measurement.

We will focus on the following form of a LGI:

$$\mathcal{C}_{i,j}(t_2-t_1)+\mathcal{C}_{i,j}(t_3-t_2)-\mathcal{C}_{i,j}(t_3-t_1)\leqslant 1, \tag{23}$$

where $\mathcal{C}_{i,j}(t_\alpha,t_\beta)$ is a two-time correlation [see Eq. (6)] of the qubit nonlocal Majorana operator $\hat{Q}_{i,j}$ (with eigenvalues ±1) between times t_α and t_β and $t_1<t_2<t_3$. We concentrate on the case of identical time intervals, i.e., $t_2-t_1=t_3-t_2=t$, defining a LGI function $\mathcal{K}_{i,j}(t)$ as [37]

$$\mathcal{K}_{i,j}(t)=2\mathcal{C}_{i,j}(t)-\mathcal{C}_{i,j}(2t)\leqslant 1. \tag{24}$$

Like the Bell inequality test, any system that violates this LGI can be guaranteed to behave in a nonclassical sense. From now on, we will take larger violations of the LGI as an indication that a system has more quantum characteristics than another one.

Figure 5 displays the evolution, as a function of Δt, of the LGI function $\mathcal{K}_{i,j}(t)$ given by Eq. (24) for the same parameters as used in Fig. 4. We first note that the inequality is always violated at very early times, a result that can be already understood from the $O(t^2)$ expansions given in Eqs. (8) and (9). Specifically, the $\mathcal{C}_1^{(x)}(t)$-TTC-based LGI, denoted by $\mathcal{K}_1^{(x)}(t)$, is given by

$$\mathcal{K}_1^{(x)}(t)\simeq 1+\mu^2t^2+O(t^4), \tag{25}$$

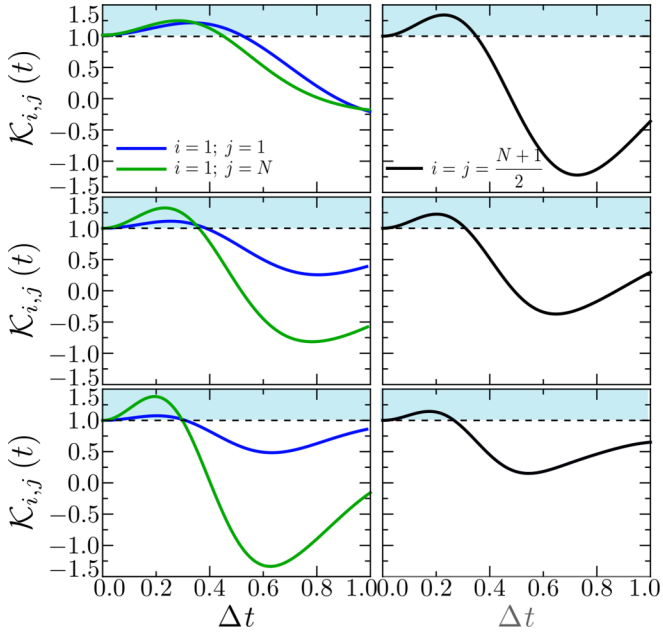

FIG. 5. Two-Majorana $\mathcal{K}_{i,j}(t)$ LGI function as a function of Δt. Panels and colored lines have the same meaning as in Fig. 4. The upper blue zones represent violations of the LGI given by Eq. (24).

while that based on $\mathcal{C}_1^{(z)}(t)$, denoted by $\mathcal{K}_1^{(z)}(t)$, is

$$\mathcal{K}_1^{(z)}(t) \simeq 1 + 4\Delta^2 t^2 + O(t^4). \tag{26}$$

Thus, the initial growth of both inequality violations is captured again by the universal initial curvatures of the corresponding TTCs. Furthermore, the early-time violations for $\mathcal{K}_1^{(x)}(t)$ and $\mathcal{K}_1^{(z)}(t)$ become identical at $\mu = 2\Delta$, i.e., the critical point. This conclusion provides an alternative route to identifying the topological phase transition.

Now we consider different inequalities for longer times. It is evident that LGI functions based on local two-Majorana TTCs such as edge $\mathcal{C}_{1,1}(t)$ and bulk $\mathcal{C}_{\frac{N+1}{2},\frac{N+1}{2}}(t)$ follow a similar trend, which is very different from that of the nonlocal two-Majorana TTC given by $\mathcal{C}_{1,N}(t)$ when crossing from one phase to the other. The local LGI violations turn out to be stronger in the topological phase, while the nonlocal LGI violation increases when going from the topological to the trivial phase. This contrasting behavior can also be seen in Fig. 6, where we compare the maximum LGI violation $\mathcal{K}_{\rm Max}(\mu)$ as a function of μ (left panel) for single- and double-Majorana qubits, as well as the times for which that maximum violation occurs $t_{\mathcal{K}_{\rm Max}}(\mu)$ for the same qubits (right panel). Interestingly, for the nonlocal edge two-Majorana case, the second derivative of $\mathcal{K}_{\rm Max}(\mu)$ with respect to μ shows a dip signaling the phase transition, again a feature inherited from the corresponding time correlations $\mathcal{C}_{1,N}(t)$ (see Fig. 1). Thus, we can conclude that LGI violations by nonlocal Majorana qubits are sensitive to the topological features of the underlying phase, and consequently, they could be explored in properly designed experimental setups.

V. EXPERIMENTAL IMPLEMENTATIONS

Among the most promising candidates for experimentally detecting Majorana edge fermions in condensed-matter sys-

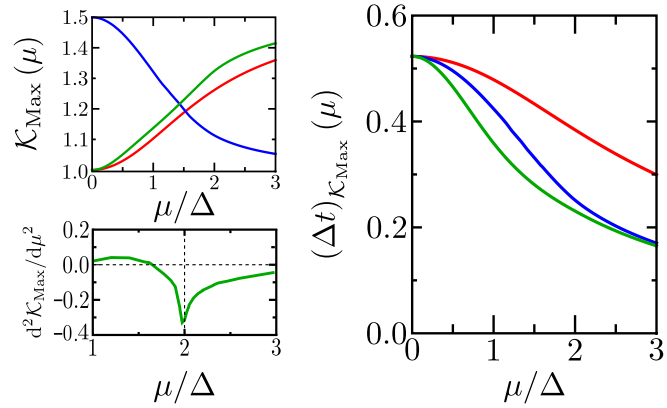

FIG. 6. Top left: maximum violation of LGI as a function of μ/Δ. Right: time of maximum LGI violation as a function of μ/Δ. Bottom left: second derivative of the maximum LGI violation with respect to μ showing a dip signaling the phase transition for the nonlocal edges two-Majorana case. Red lines depict the $\mathcal{C}_1^{(x)}(t)$-TTC-based LGI, the blue lines represent the $\mathcal{C}_1^{(z)}(t)$-TTC-based LGI, and the green lines correspond to $\mathcal{C}_{1,N}(t)$-TTC-based LGI.

tems are chains of magnetic atoms on superconducting surfaces [4,5,50] and semiconducting nanowires with large Rashba spin-orbit interaction under an applied magnetic field and induced superconductivity by proximity effects [51,52]. Previous works have focused on local sensitive tunneling signatures of the topological phase transition in the boundary fermion occupation (Kitaev chain) or boundary spin (transverse field Ising chain).

In the Rashba nanowire setup Sticlet *et al.* [51] defined local Majorana pseudospins and argued that they could be measured by spin-polarized STM, allowing one to directly visualize the Majorana fermionic states and to test the topological character of the 1D system. On the other hand, Deng *et al.* [53] reported that highly sensitive experiments were recently conducted in which the nonlocality of Majorana qubits can be *locally* probed by a quantum dot at one end of the nanowire. These state-of-the-art experiments could evolve to develop time-dependent sensitivity as required for detecting local and nonlocal TTCs. Recently, there has been great interest in contrasting distinctive signatures of spin polarization for Andreev and Majorana bound states [54] since, when identifying topological phases, effects resulting from the presence of quasiparticle states inside the superconducting gap should be carefully eliminated [55]. Thus, it is most desirable to have additional signatures available (besides tunneling conductance signatures of Majorana fermions) that would allow one to identify the topological phase transition. References [51,53] have proposed how to distinguish such differences between Andreev and Majorana signatures by accessing true nonlocal features. In this way, our results as given by the behavior of local $\mathcal{C}_1^{(x)}(t)$ and, most importantly, by nonlocal $\mathcal{C}_{1,N}(t)$ and their LGI combinations should be relevant for extending that kind of search for true Majorana behavior.

Furthermore, recently, spin noise spectroscopy was shown to be a powerful tool to experimentally access the autocorrelation function [56,57]. The universal short-time behavior described by Eqs. (7) and (8) could be exploited in spin fluctuation

measurements as an alternative route to get information about the dynamics [58]. Such a rich variety of behaviors would also permit the study of temporal effects as well as different kinds of susceptibilities, through their Fourier transform equivalents, in topological quantum computing settings.

Therefore, in light of recent experiments, we demonstrate in the present work that TTC and LGI behaviors exhibit a quantum-phase-sensitive signature due to the appearance of zero-energy modes in the topological phase that will manifest themselves in the long-time behavior of both local and nonlocal qubit TTCs. This provides an experimentally useful diagnostic tool to detect topological phase transitions.

VI. CONCLUDING REMARKS

In summary, we have provided evidence that time correlations and violations of LGIs establish new testable signatures of topological phase transitions. The behavior of that sort of inequality is a direct consequence of time correlations in local and nonlocal Majorana qubits. Specifically, we have identified signatures of the Majorana fermion chain topological phase transition in three time domains: (i) In the short-time limit we found universal features such as the out-of-time-ordered correlation and a dip in the second μ derivative marking the phase transition. (ii) In the intermediate-time region, the LGI violations are sensitive to the quantum phase of the system. (iii) Finally, in the long-time limit, the asymptotic values of single- and double-Majorana edge TTCs act as order-parameter-like indicators. Specifically, we proposed that a measurement of the long-time saturation value of the local edge $\mathcal{C}_1^{(x)}$ TTC as well as the nonlocal edge $\mathcal{C}_{1,N}$ TTC provides a witness of the topological ($\neq 0$) vs nontopological ($=0$) phase transition of Majorana fermion chain systems, as it directly probes the existence of zero-energy modes. Additionally, in the former case it gives direct access to the electron-hole weight of such modes. The results are especially relevant because the whole question of quantum coherence in complex mesoscopic systems is taking up a new impulse in the community and is of interest to researchers not only of quantum information and foundations but also of condensed matter.

ACKNOWLEDGMENTS

F.J.G.-R., J.J.M.-A., F.J.R., and L.Q. acknowledge financial support from Vicerrectoría de Investigaciones through UniAndes-2015 project "Quantum control of nonequilibrium hybrid systems-Part II." F.J.G.-R. and F.J.R acknowledge financial support from Facultad de Ciencias at Universidad de los Andes (2018-I). C.T. acknowledges support from the Spanish MINECO under Contracts No. MAT2014-53119-C2-1-R and No. MAT2017-83722-R. We acknowledge financial support from the project CEAL-AL/2017-25 UAM-Banco Santander for a collaboration between the Universidad Autónoma de Madrid and the Universidad de los Andes in Bogotá. L.Q. thanks UAM for kind hospitality. F.J.G.-R. thanks the University of Massachusetts Boston for kind hospitality.

[1] J. Alicea, Y. Oreg, G. Refael, F. von Oppen, and M. P. A. Fisher, Nat. Phys. **7**, 412 (2011).
[2] S. D. Sarma, M. Freedman, and C. Nayak, npj Quantum Inf. **1**, 15001 (2015).
[3] J. D. Sau, R. M. Lutchyn, S. Tewari, and S. Das Sarma, Phys. Rev. B **82**, 094522 (2010).
[4] S. Nadj-Perge, I. K. Drozdov, J. Li, H. Chen, S. Jeon, J. Seo, A. H. MacDonald, B. A. Bernevig, and A. Yazdani, Science **346**, 602 (2014).
[5] K. Halterman and M. Alidoust, Phys. Rev. B **94**, 064503 (2016).
[6] K. K. Tanaka, M. Ichioka, and S. Onari, Phys. Rev. B **93**, 094507 (2016).
[7] G. Moore and N. Read, Nucl. Phys. B **360**, 362 (1991).
[8] R. M. Lutchyn, J. D. Sau, and S. Das Sarma, Phys. Rev. Lett. **105**, 077001 (2010).
[9] V. Mourik, K. Zuo, S. M. Frolov, S. R. Plissard, E. P. A. M. Bakkers, and L. P. Kouwenhoven, Science **336**, 1003 (2012).
[10] A. Das, Y. Ronen, Y. Most, Y. Oreg, M. Heiblum, and H. Shtrikman, Nat. Phys. **8**, 887 (2012).
[11] E. Dumitrescu, B. Roberts, S. Tewari, J. D. Sau, and S. Das Sarma, Phys. Rev. B **91**, 094505 (2015).
[12] S. R. Elliott and M. Franz, Rev. Mod. Phys. **87**, 137 (2015).
[13] D. J. Clarke, J. D. Sau, and S. Das Sarma, Phys. Rev. X **6**, 021005 (2016).
[14] R. Aguado, La Rivista del Nuovo Cimento **40**, 523 (2017).
[15] S. M. Albrecht, A. P. Higginbotham, M. Madsen, T. S. Jespersen, J. Nygard, P. Krogstrup, and C. M. Marcus, Nature (London) **531**, 206 (2016).
[16] L. Kuerten, C. Richter, N. Mohanta, T. Kopp, A. Kampf, J. Mannhart, and H. Boschker, Phys. Rev. B **96**, 014513 (2017).
[17] Y. Kalcheim, O. Millo, A. Di Bernardo, A. Pal, and J. W. A. Robinson, Phys. Rev. B **92**, 060501 (2015).
[18] M. Alidoust and K. Halterman, Phys. Rev. B **97**, 064517 (2018).
[19] M. Alidoust, K. Halterman, and O. T. Valls, Phys. Rev. B **92**, 014508 (2015).
[20] M. Alidoust, A. Zyuzin, and K. Halterman, Phys. Rev. B **95**, 045115 (2017).
[21] N. Brunner, D. Cavalcanti, S. Pironio, V. Scarani, and S. Wehner, Rev. Mod. Phys. **86**, 419 (2014).
[22] D. E. Drummond, A. A. Kovalev, C.-Y. Hou, K. Shtengel, and L. P. Pryadko, Phys. Rev. B **90**, 115404 (2014).
[23] M. Gessner, M. Ramm, H. Häffner, A. Buchleitner, and H.-P. Breuer, Europhys. Lett. **107**, 40005 (2014).
[24] M. Gessner, M. Ramm, T. Pruttivarasin, A. Buchleitner, H.-P. Breuer, and H. Häffner, Nat. Phys. **10**, 105 (2013).
[25] A. Y. Kitaev, Phys. Usp. **44**, 131 (2001).
[26] A. J. Leggett and A. Garg, Phys. Rev. Lett. **54**, 857 (1985).
[27] A. J. Leggett, Rep. Prog. Phys. **71**, 022001 (2008).
[28] C. Emary, N. Lambert, and F. Nori, Rep. Prog. Phys. **77**, 016001 (2014).
[29] A. Palacios-Laloy, F. Mallet, F. Nguyen, P. Bertet, D. Vion, D. Esteve, and A. N. Korotkov, Nat. Phys. **6**, 442 (2010).
[30] M. E. Goggin, M. P. Almeida, M. Barbieri, B. P. Lanyon, J. L. O'Brien, A. G. White, and G. J. Pryde, Proc. Natl. Acad. Sci. U.S.A. **108**, 1256 (2011).

[31] G. C. Knee, S. Simmons, E. M. Gauger, J. J. Morton, H. Riemann, N. V. Abrosimov, P. Becker, H.-J. Pohl, K. M. Itoh, M. L. Thewalt, G. A. D. Briggs, and S. C. Benjamin, Nat. Commun. **3**, 606 (2012).
[32] V. Athalye, S. S. Roy, and T. S. Mahesh, Phys. Rev. Lett. **107**, 130402 (2011).
[33] G. Waldherr, P. Neumann, S. F. Huelga, F. Jelezko, and J. Wrachtrup, Phys. Rev. Lett. **107**, 090401 (2011).
[34] J. Dressel, C. J. Broadbent, J. C. Howell, and A. N. Jordan, Phys. Rev. Lett. **106**, 040402 (2011).
[35] T. White, J. Mutus, J. Dressel, J. Kelly, R. Barends, E. Jeffrey, D. Sank, A. Megrant, B. Campbell, Y. Chen, Z. Chen, B. Chiaro, A. Dunsworth, I.-C. Hoi, C. Neill, P. O'Malley, P. Roushan, A. Vainsencher, J. Wenner, A. N. Korotkov, and J. M. Martinis, npj Quantum Inf. **2**, 15022 (2016).
[36] E. Huffman and A. Mizel, Phys. Rev. A **95**, 032131 (2017).
[37] F. J. Gómez-Ruiz, J. J. Mendoza-Arenas, F. J. Rodríguez, C. Tejedor, and L. Quiroga, Phys. Rev. B **93**, 035441 (2016).
[38] N. Lambert, C. Emary, Y.-N. Chen, and F. Nori, Phys. Rev. Lett. **105**, 176801 (2010).
[39] M. Lee, S. Han, and M.-S. Choi, New J. Phys. **18**, 063004 (2016).
[40] See Supplemental Material at http://link.aps.org/supplemental/10.1103/PhysRevB.97.235134 for details of the calculations and derivations.
[41] B. Narozhny, Sci. Rep. **7**, 1447 (2017).
[42] B. Swingle, G. Bentsen, M. Schleier-Smith, and P. Hayden, Phys. Rev. A **94**, 040302 (2016).
[43] H. Shen, P. Zhang, R. Fan, and H. Zhai, Phys. Rev. B **96**, 054503 (2017).
[44] M. Gärttner, J. G. Bohnet, A. Safavi-Naini, M. L. Wall, J. J. Bollinger, and A. M. Rey, Nat. Phys. **13**, 781 (2017).
[45] J. Li, R. Fan, H. Wang, B. Ye, B. Zeng, H. Zhai, X. Peng, and J. Du, Phys. Rev. X **7**, 031011 (2017).
[46] O. Dmytruk, M. Trif, and P. Simon, Phys. Rev. B **92**, 245432 (2015).
[47] V. Kostov, A. Martinez-Finkelshtein, and B. Shapiro, J. Approximation Theory **161**, 464 (2009).
[48] T. Mansour and Y. Sun, Discrete Math. **309**, 4079 (2009).
[49] J. Kemp, N. Y. Yao, C. R. Laumann, and P. Fendley, J. Stat. Mech. (2017) 063105.
[50] J. Li, S. Jeon, Y. Xie, A. Yazdani, and B. A. Bernevig, Phys. Rev. B **97**, 125119 (2018).
[51] D. Sticlet, C. Bena, and P. Simon, Phys. Rev. Lett. **108**, 096802 (2012).
[52] M. M. Maśka, A. Gorczyca-Goraj, J. Tworzydło, and T. Domański, Phys. Rev. B **95**, 045429 (2017).
[53] M. T. Deng, S. Vaitiekénas, E. Prada, P. San-Jose, P. Nygård, J. Krogstrup, R. Aguado, and C. M. Marcus, arXiv:1712.03536.
[54] K. Zhang, J. Zeng, Y. Ren, and Z. Qiao, Phys. Rev. B **96**, 085117 (2017).
[55] C.-H. Lin, J. D. Sau, and S. Das Sarma, Phys. Rev. B **86**, 224511 (2012).
[56] N. A. Sinitsyn and Y. V. Pershin, Rep. Prog. Phys. **79**, 106501 (2016).
[57] F. J. Burnell, A. Shnirman, and Y. Oreg, Phys. Rev. B **88**, 224507 (2013).
[58] F. J. Burnell, Phys. Rev. B **89**, 224510 (2014).